Journal of Biomechanics 48 (2015) 1264–1269

Contents lists available at ScienceDirect

Journal of Biomechanics

journal homepage: www.elsevier.com/locate/jbiomech
www.JBiomech.com

Theoretical effects of fully ductile versus fully brittle behaviors of bone tissue on the strength of the human proximal femur and vertebral body

Shashank Nawathe [a,*], Haisheng Yang [b], Aaron J. Fields [c], Mary L. Bouxsein [d], Tony M. Keaveny [a,e,1]

[a] Department of Mechanical Engineering, University of California, Berkeley, CA, USA
[b] Department of Basic Medical Sciences, Purdue University, IN, USA
[c] Department of Orthopaedic Surgery, University of California, San Francisco, CA, USA
[d] Beth Israel Deaconess Medical Center, Boston, MA, USA
[e] Department of Bioengineering, University of California, Berkeley, CA, USA

ARTICLE INFO

Article history:
Accepted 28 February 2015

Keywords:
Tissue-level ductility
Femur
Microstructure
Whole bone
Fracture

ABSTRACT

The influence of the ductility of bone tissue on whole-bone strength represents a fundamental issue of multi-scale biomechanics. To gain insight, we performed a computational study of 16 human proximal femurs and 12 T9 vertebral bodies, comparing the whole-bone strength for the two hypothetical bounding cases of fully brittle versus fully ductile tissue-level failure behaviors, all other factors, including tissue-level elastic modulus and yield stress, held fixed. For each bone, a finite element model was generated (60–82 μm element size; up to 120 million elements) and was virtually loaded in habitual (stance for femur, compression for vertebra) and non-habitual (sideways fall, only for femur) loading modes. Using a geometrically and materially non-linear model, the tissue was assumed to be either fully brittle or fully ductile. We found that, under habitual loading, changing the tissue behavior from fully ductile to fully brittle reduced whole-bone strength by 38.3 ± 2.4% (mean ± SD) and 39.4 ± 1.9% for the femur and vertebra, respectively ($p=0.39$ for site difference). These reductions were remarkably uniform across bones, but (for the femur) were greater for non-habitual (57.1 ± 4.7%) than habitual loading ($p<0.001$). At overall structural failure, there was 5–10-fold less failed tissue for the fully brittle than fully ductile cases. These theoretical results suggest that the whole-bone strength of the proximal femur and vertebra can vary substantially between fully brittle and fully ductile tissue-level behaviors, an effect that is relatively insensitive to bone morphology but greater for non-habitual loading.

1. Introduction

The post-yield ductility of bone tissue, which is associated primarily with its organic components and enables the tissue to deform and take load beyond the elastic range, varies substantially across and within vertebrates. Bone tissue from the tympanic bulla in fin whales is highly brittle whereas bone tissue from the antler in red deer can sustain extremely large deformations before fracturing (Currey, 2002); and human bone lies somewhere in between (Hernandez et al., 2005; McCalden et al., 1993; Reilly and Burstein, 1975). One poorly understood issue is how tissue-level post-yield ductility per se influences the organ level strength of the bone—independent of other key bone-strength factors, such as bone mineral content, bone geometry, and microstructure, as well as the elastic and yield material properties of the tissue. This is a particularly challenging problem for structurally complex bones that contain both trabecular bone and thin cortices, such as the proximal femur and vertebra. From an evolutionary biomechanics perspective, understanding the relation between tissue-level post-yield ductility and whole-bone strength might provide insight into how bones evolved. This relation is also of interest clinically as tissue-level ductility can be very low in certain bone pathologies, e.g. *osteogenesis imperfecta*, and it has been proposed that subtle variations in tissue post-yield ductility may play a role in age-related bone fragility and the etiology of osteoporotic hip fractures (Ammann and Rizzoli, 2003; Turner, 2002).

* Corresponding author. Tel.: +1 510 508 1263.
E-mail addresses: shashank@berkeley.edu, nawathe.shashank@gmail.com (S. Nawathe), tmk@me.berkeley.edu (T.M. Keaveny).
[1] 6175 Etcheverry Hall, University of California, Berkeley, CA 94720-1740, USA. Tel: +1 510 642 8017; fax: +1 510 642 6163.

http://dx.doi.org/10.1016/j.jbiomech.2015.02.066
0021-9290/

While the relation between tissue-level post-yield ductility at one physical scale and strength of the bone at some higher scale has recently been investigated for small specimens of trabecular bone (Nawathe et al., 2013), and while this relation is relatively well understood for structurally simple diaphyseal-type bones composed only of cortical bone (Beer et al., 2006), little is known regarding the relation between whole-bone strength and tissue-level ductility in more complex whole bones such as the proximal femur and vertebral body, nor the magnitude of this effect. This multi-scale biomechanics problem is confounded by the vast heterogeneity in whole-bone geometry and morphology across the population (Bell et al., 1999; Fazzalari et al., 2006; Keaveny et al., 2010; Mosekilde and Mosekilde 1990). Further, the interaction between the cortical and trabecular compartments and the type of external loading can alter the underlying micro-mechanics (Nawathe et al.; van Rietbergen et al., 2003; Verhulp et al., 2008) and therefore might mediate the relationship between tissue-level ductility and whole-bone strength.

Addressing these challenges, we utilized non-linear finite element analyses of a cohort of human proximal femurs and vertebrae to investigate how, in theory, whole-bone strength is altered when the tissue-level post-yield deformation is changed from being fully ductile to fully brittle—the two hypothetical bounds of tissue-level post-yield ductility. Computer simulations make it feasible to quantitatively assess the effects of tissue-level ductility on whole-bone strength in a precise repeated-measures manner, which is not possible solely with experimentation due to the difficulty of altering tissue-level post-yield ductility in a controlled fashion as well as the destructive nature of any physical strength testing. In this way, we provide estimates of the bounds of the influence of tissue-level post-yield ductility per se on whole-bone strength, accounting for most other factors that influence bone strength.

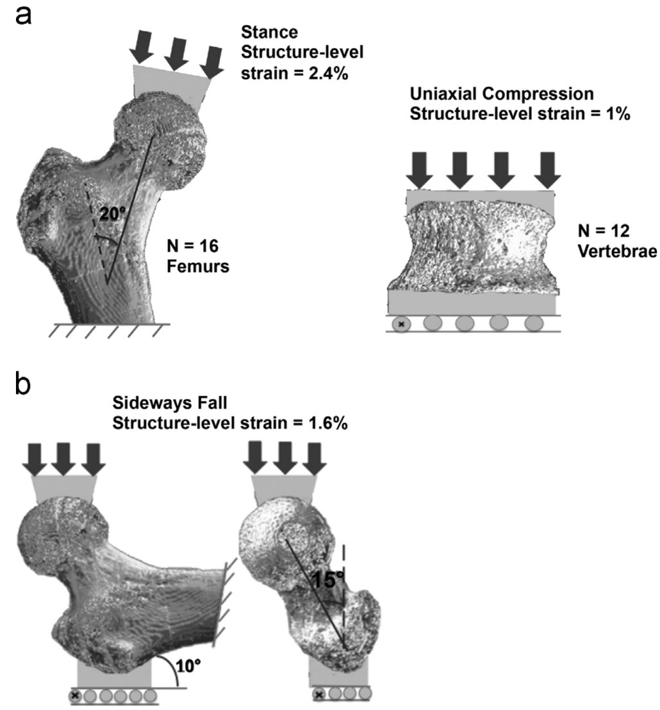

Fig. 1. Boundary conditions used to simulate: (a) habitual loading, for the femurs and vertebrae, and (b) non-habitual loading, only for the femurs. Habitual loading: stance loading of the femur and uniaxial compression loading of the vertebra; non-habitual loading: a sideways fall on the greater trochanter of the femur. A virtual layer of polymethyl methacrylate (PMMA; E=2500 MPa) was used to distribute loads evenly.

2. Materials and methods

2.1. Specimen preparation and imaging

This investigation was performed on sixteen human proximal femurs (age=76 ± 10 years, range=62–93 years; n=12 female, n=4 male) and twelve thoracic ninth (T9) vertebral bodies (age=77 ± 11 years; n=3 female, n=9 male) that were obtained fresh-frozen from cadavers, with no medical history of metabolic bone disorders. High-resolution images were acquired of each intact femur (XtremeCT; isotropic voxel size of 61.5-μm, Scanco Medical AG; Brüttisellen, Switzerland) and vertebra (micro-CT, isotropic voxel size of 30-μm, Scanco Medical AG; Brüttisellen, Switzerland). Using a volume-preserving coarsening routine and a bone-specific global threshold value, the femur and vertebra images were coarsened to 82-μm and 60-μm voxel size, respectively, to facilitate computational analysis. The trabecular and cortical compartments within the whole bones were also identified (Eswaran et al., 2006; Nawathe et al., 2014) using a two-dimensional ray-based search algorithm (IDL software suite, ITT Visual Information Solutions, Boulder, CO, USA).

2.2. Finite element modeling

Some of the bones included in this analysis were used in previous analyses (Fields et al., 2012; Nawathe et al., 2014; Yang et al., 2012). Finite element models were created from the images by converting each coarsened image voxel directly into an 8-noded cube-shaped finite element (van Rietbergen et al., 1995). The finite element models for the proximal femur had up to 120 million elements and those of the vertebra had up to 70 million elements. Two different types of loading conditions were implemented—one to simulate habitual loading (femur and spine) and the other non-habitual loading (femur only). For the habitual loading (Fig. 1(a)), we used displacement boundary conditions to simulate stance loading for the femur (Keyak et al., 2001) and uniform compression for the vertebral body (Fields et al., 2012). For the non-habitual loading (Fig. 1(b), only performed for the femur), we simulated a 15° sideways fall on the greater trochanter (Nawathe et al., 2014). All loads were applied through a virtual layer of polymethylmethacrylate (E=2500 MPa) in order to distribute the loads evenly over the bone surfaces.

For both the hip and spine, all elements were assigned the same tissue-level elastic and yield properties. The isotropic elastic modulus of 7.3 GPa (Nawathe et al., 2014) was initially calibrated by comparing the finite element-estimated vs. experimental measures of femoral strength for n=12 femurs (R^2=0.94), and was then verified using n=6 additional femurs (R^2=0.92). We used a Poisson's ratio of 0.3, and yield strains of 0.81% in compression and 0.33% in tension, respectively (Bayraktar et al., 2004). For all analyses, kinematic large-deformation geometric non-linearity was included in the constitutive model (Bevill et al., 2006; Stolken and Kinney, 2003). For computational efficiency, the bone tissue in the superior portion of the femoral head was not allowed to fail so as to eliminate spurious stress oscillations near the boundary conditions. For these models, we have previously reported a high correlation (R^2=0.94 for femurs and R^2=0.85 for vertebra) between the finite element-estimated and experimentally determined measures of whole-bone strength (Fields et al., 2012; Nawathe et al., 2014), which supports the validity of our modeling approach.

For each model, two separate non-linear finite element analyses were performed to simulate two hypothetical bounding cases of post-yield behavior, namely fully brittle and fully ductile tissue-level failure behaviors (Fig. 2). For the fully ductile case (Fig. 2(a)), we assumed tissue-level failure by yielding, using a rate-independent elasto-plasticity model (Papadopoulos and Lu, 1998) comprised of a modified von-Mises criterion with tension-compression strength asymmetry (Bayraktar et al., 2004; Niebur et al., 2000). In this analysis, the bone tissue can only yield, it never fractures, and there is no limit on the magnitude of the post-yield tissue-level strains. For the fully brittle case (Fig. 2(b)), tissue-level fracture is assumed to occur once the yield stress (in either tension or compression) is exceeded. We used a quasi-nonlinear approach to simulate this type of brittle fracture. In particular, an elastic but geometrically non-linear analysis was performed to a specified level of whole-bone strain; stresses were computed at each element centroid, as was the overall structure-level reaction force at the femoral head. This reaction force was used as a single point on the overall force–deformation (strain) curve. Then the maximum and minimum principal stresses at each element centroid were checked to identify if any exceeded the assumed respective tissue-level tensile or compressive yield strengths, and if so, that element was assumed to crack or fracture—and its tensile or compressive failure mode was noted—and its elastic modulus (and thus yield strength) was reduced 100-fold for subsequent analyses. Using these reduced properties in all such "fractured" elements, a new analysis was then performed for the whole specimen, but loaded now (from zero load) to an incrementally higher structure-level strain, producing a new value for the overall structure-level reaction force. This whole process was repeated until we generated an overall structure-level force–strain curve that displayed an ultimate point, defined by a reduction in the overall structure-level reaction force.

Substantial computational infrastructure was required to perform the overall analysis. Each finite element model contained up to 400 million degrees of freedom, and was solved using an implicit, parallel finite element framework (Adams et al., 2004). Computer simulations were performed on the supercomputing resources (Stampede and Ranger) available at the Texas Advanced Computing Center (TACC). TACC Stampede system is a 10 PFLOPS (PF) Dell Linux Cluster based on 6400+ Dell PowerEdge server nodes, wherein the compute nodes are configured with two Xeon